AIP | Applied Physics Letters

Robust sensing methodology for detecting change with bistable circuitry dynamics tailoring

R. L. Harne and K. W. Wang

Citation: Appl. Phys. Lett. **102**, 203506 (2013); doi: 10.1063/1.4807772
View online: http://dx.doi.org/10.1063/1.4807772
View Table of Contents: http://apl.aip.org/resource/1/APPLAB/v102/i20
Published by the American Institute of Physics.

Robust sensing methodology for detecting change with bistable circuitry dynamics tailoring

R. L. Harne[a] and K. W. Wang
Department of Mechanical Engineering, University of Michigan, Ann Arbor, Michigan 48109, USA

(Received 6 April 2013; accepted 11 May 2013; published online 22 May 2013)

In contrast to monitoring natural frequency shift, bifurcation-based sensing techniques utilize dramatic switches in response amplitude to detect structural change. We demonstrate a highly sensitive bifurcation-based sensing method requiring only the monitored structure, a transduction mechanism, and bistable electric circuitry. The system configuration is broadly applicable from, e.g., microscale mass sensing to structural health monitoring. In contrast to single bifurcation events of past techniques, the present methodology introduces new bifurcations that may be utilized sequentially for monitoring numerous thresholds of structural parameter change. We show that bifurcation-based sensing potential and versatility is greatly advanced. © *2013 AIP Publishing LLC*. [http://dx.doi.org/10.1063/1.4807772]

Many vibration-based sensing methodologies translate shift in system natural frequency to an influence upon or within the system due to an identifiable parameter change. This approach is broadly applicable from detecting biological or chemical mass adsorption on vibrating microelectromechanical systems (MEMS)[1] to monitoring the viability of mechanical and civil structures.[2,3] Employing dynamic principles similar to Josephson bifurcation amplifiers,[4] recent works in MEMS mass sensing have demonstrated more sensitive techniques based upon nonlinear phenomena including parametric resonance[5–7] and softening Duffing oscillator saddle node bifurcation.[8,9] These bifurcation-based methods yield significant response amplitude jumps in consequence to small system perturbations thus dramatically reducing the mass adsorption necessary for unambiguous detection. While monitoring, natural frequency shift is limited by analog features related to hardware performance, detecting change via bifurcation is a digital metric having fundamental resolution ideally governed only by noise thresholds.[4] Since bifurcation-based sensing may use constant frequency excitation, additional hardware necessary to track a shifting natural frequency is favorably obviated.

While demonstrations of bifurcation-based sensing for MEMS are so far promising, there are limitations to be resolved. Chief among these are the reusability of some sensors following bifurcation dynamics;[8] the repeatability of bifurcation frequency if crossed numerous times[9] that may be influenced by mass adsorption rate (or sweep rate during characterization[6]); the potential for fatigue failure when operating a structure so as to continually transit between large and small vibrations; and limited bifurcation utility when employing softening Duffing systems. Since bifurcation phenomena require considerable nonlinearity to provide enhanced detection sensitivity, the approaches have thus far been applied only for micro- and smaller-scale systems where nonlinear dynamics are prevalent.[10] To alleviate these concerns and greatly enhance the range of applicability and versatility of bifurcation-based sensing, we demonstrate a more encompassing system design and tailorable sensing methodology employing bistable dynamics. Consequently, the approach is as applicable to MEMS mass sensing as it is to full-scale structural health monitoring. The sensing componentry is the combination of an electromechanical element and bistable electric circuit; this simplifies overall system fabrication by requiring only linear mechanical dynamics which thereafter serve as stimulus for bistable circuit bifurcation crossing. By utilizing a bistable as compared to softening Duffing system, we introduce new bifurcation phenomena providing opportunity to detect numerous, discrete, and tailorable thresholds of parameter change. The monitored structure and transducer components may be realized in practice, e.g., by a piezoelectric MEMS resonator or by applying a piezoelectric patch to a mechanical or civil structure which are both common integrations in the applications referenced above.[9,11] The output from the transducer becomes the bistable circuit input, schematically illustrated in Fig. 1 for a monitored beam having piezoelectric patch near the clamped support. One piezoelectric electrode lead connects to input resistance R_i and the bistable circuit input, while the other lead contacts common ground.

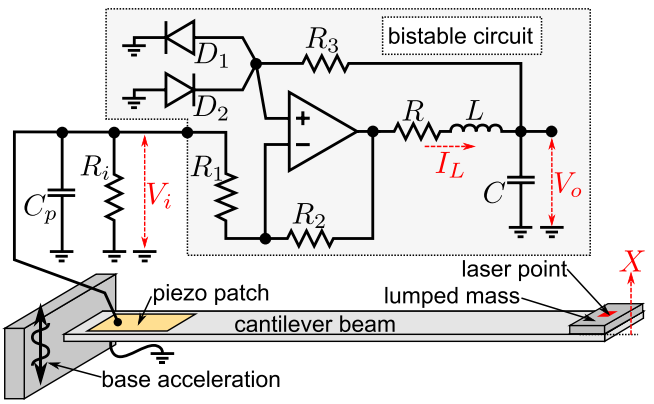

FIG. 1. Experimental configuration: base-excited cantilevered beam with tip mass and piezoelectric patch having electrode leads connected to ground and bistable circuit.

[a]Author to whom correspondence should be addressed. Electronic mail: rharne@umich.edu

Unlike past bifurcation-based sensing approaches utilizing softening Duffing oscillators in a *bistable dynamic* regime,[8,9] a classically defined bistable system exhibits two *static* equilibria between which is an unstable equilibrium. A bistable system exhibits two primary vibrational responses: low-energy, intrawell oscillations around one stable equilibrium, or high-energy, interwell vibrations when the system snaps back and forth across the unstable equilibrium position. In the proposed system design, the bistable circuit is only excited by the transducer and does not backwards-couple with electromechanical dynamics; consequently, change in monitored structural parameters yields only a variation of input voltage (excitation level) to the circuit. Fig. 2 plots the response amplitude dependence on excitation level of a harmonically excited bistable system at two frequencies, computed from earlier analysis.[12] In Fig. 2(a), small intrawell oscillations near point D are destabilized due to incremental increase in excitation level (corresponding to structural parameter change), leading to high amplitude interwell vibrations, point E. Likewise, operation near bifurcation jump G-H provides opportunity to detect a small parameter change via dramatic drop in response amplitude from inter- to intrawell oscillations. In this work, we demonstrate the *sequential* utilization of bifurcations exemplified by jumps D-E and G-H, not only to detect small accumulation of mass upon the monitored structure near the transition points themselves but also to *passively* indicate net parameter change via sequential jumps. Passive determination of net parameter variation via successive bifurcations has yet to be explored and bistable dynamics uniquely offer opportunity for this enhanced capability. Moreover, by operation at a different frequency, three response amplitude curves may be obtained, Fig. 2(b), for two-stage jumps up and/or down likewise capable successive operation. By employing a classically defined bistable element, multi-jump trajectories significantly extend the versatility of bifurcation-based sensing from existing benchmarks.[5–9]

These are the responses we aim to utilize for enhanced bifurcation-based sensing. The bistable circuit depicted in Fig. 1 was recently synthesized[13] and shown to exhibit chaotic responses characteristic of the Duffing-Holmes oscillator[14] when excited by controlled input voltage V_i, indicating the dynamic similarity between the circuit and classical bistable mechanical system. Assuming a single-mode approximation of the structural response[15] and ideal op-amp and diode characteristics, we obtain governing equations for the system of Fig. 1

$$\dot{\mathbf{x}} = \begin{bmatrix} 0 & 1 & 0 & 0 & 0 \\ -k/m & -b/m & -\theta/m & 0 & 0 \\ 0 & \theta/C_p & -1/R_iC_p & 0 & 0 \\ 0 & 0 & 0 & 0 & 1/C \\ 0 & 0 & 1/L & 0 & -R/L \end{bmatrix} \mathbf{x} - \begin{bmatrix} 0 \\ p\sin\omega t \\ 0 \\ 0 \\ F^*/L \end{bmatrix}. \tag{1}$$

Here, $\mathbf{x} = [x_1, ..., x_5]^{\mathrm{T}} = [X, \dot{X}, V_i, V_o, I_L]^{\mathrm{T}}$; m, b, and k represent structure modal mass, damping, and stiffness, respectively; p is base acceleration (or negative mass-normalized direct forcing) level; $\omega/2\pi$ is excitation frequency in Hz; θ is electromechanical coupling; C_p is piezoelectric capacitance; R_i is input load resistance; R, L, and C are bistable circuit resistance, inductance, and capacitance, respectively; and the overdot represents a time derivative. We assume $R_3 \gg \sqrt{L/C}$.[13] The voltage function F^* is piecewise linear with respect to output voltage $x_4 = V_o$ across capacitor C

$$F^*(x_4) = \begin{cases} F_1^* = x_4 + gV_d; & x_4 < -V_d \\ F_2^* = (1-g)x_4; & |x_4| \le V_d \\ F_3^* = x_4 - gV_d; & x_4 > V_d. \end{cases} \tag{2}$$

Following assumption of ideal op-amp and diodes, the feedback gain is $g = R_2/R_1 + 1$. The voltage drop over an open diode is V_d.

The piecewise linear voltage function F^*, Eq. (2), is depicted in Fig. 3 using identified experimental system parameters provided in Table I. Note that the restoring potential $U = \int F^* dx_4$ is the conjoining of three parabola and, therefore, yields the traditional bistable oscillator double-well potential.[16] As indicated in Fig. 3, the circuit is statically *and* dynamically bistable; thus, an initial circuit output voltage perturbation produces a transient dynamic response attracted to one of the two stable equilibria.

We conduct experiments with the full system depicted in Fig. 1 to validate equation system (1) so as to enable favorable tailoring of circuit design for sensing versatility based on model assumptions. The aluminum beam has length

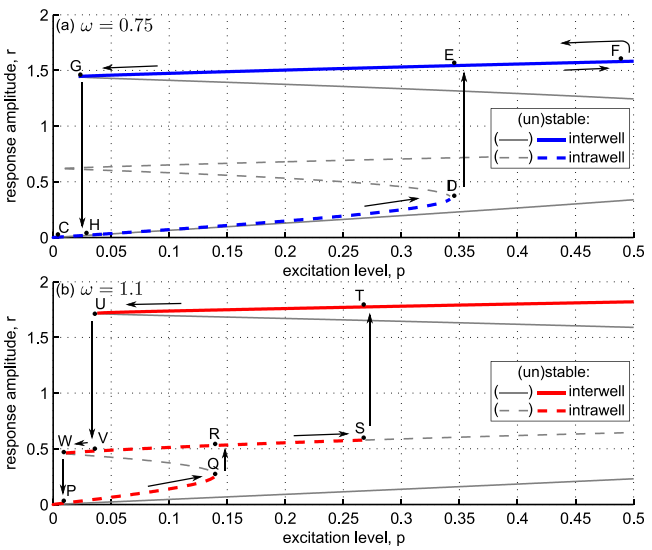

FIG. 2. Force-amplitude bifurcations computed from Eqs. (3) and (4) (Ref. 12) at (a) $\omega = 0.75$ and (b) $\omega = 1.1$. $(\gamma, \beta) = (0.02, 1)$. Arrows indicate bifurcation jump trajectories.

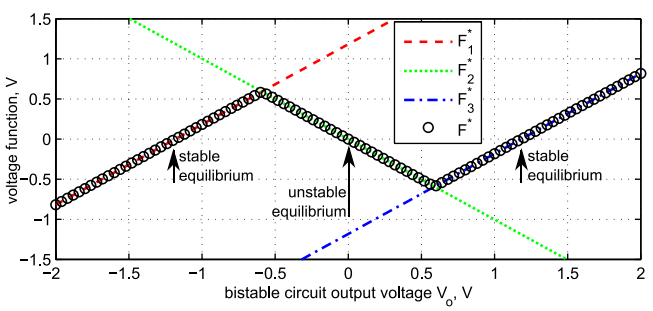

FIG. 3. Voltage function of bistable circuit.

TABLE I. Experimental system parameters.

m, g	b, N·s/m	k, N/m	θ, mN/V	C_p, nF	R_i, kΩ
65.1	0.192	252	0.135	1.65	9.71
R, Ω	L, H	C, μF	R_1, kΩ	$R_{2,3}$, kΩ	V_d, V
46.0	0.50	52.9	9.64	9.68	0.59

412 mm, width 31.6 mm, and thickness 3.15 mm. The tip mass is 38.2 g and its velocity is measured via laser vibrometer. The piezoelectric patch is an MFC M-2814-P1 by Smart Material Corp. We use 1N4148 diodes and LM741CN op-amp. The remaining parameters are given in Table I, where structural mass and stiffness are the equivalent parameters for a fundamental mode approximation;[17] damping b is determined from open-circuit ring-down responses of the beam, and electromechanical coupling θ is experimentally identified with the system disconnected from the bistable circuit and only the voltage across resistor R_i measured. The system is excited at 10 Hz with two distinct levels of base acceleration p and theoretical and experimental beam velocity $\dot{X}$ and output voltage V_o are compared in Fig. 4. The output voltage values are normalized with respect to the static equilibria voltage amplitude. Theoretical responses are predicted by directly integrating equation system (1). Fig. 4(a) shows the responses due to low input acceleration $p = 0.438\ \text{m/s}^2$. In this scenario, the bistable circuit output voltage settles into intrawell steady-state response around one of the stable equilibria. Increasing the excitation to $p = 2.17\ \text{m/s}^2$ requires the system to cross a saddle-node bifurcation that induces high-energy, interwell response during which time the output voltage crosses the unstable central equilibrium position at $V_o = 0$ once per forcing period,

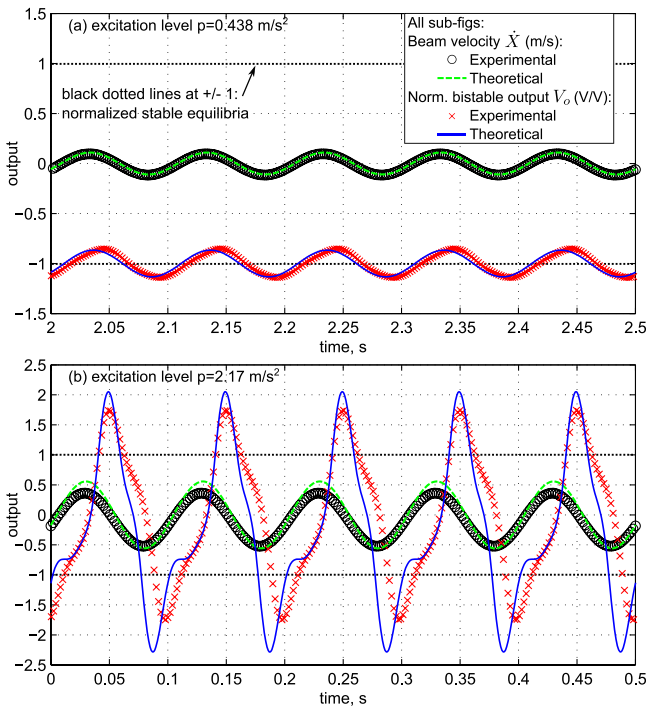

FIG. 4. Theoretical and experimental response of beam velocity and normalized bistable circuit output voltage for base accelerations (a) 0.438 m/s^2 and (b) 2.17 m/s^2.

Fig. 4(b). The theoretical results are in good quantitative agreement with measured data verifying the assumption of negligible backwards-coupling from circuit. As expected, the decoupling of responses fundamentally follows assumption (and realization) of ideal op-amp behavior. These results and observations allow us to design the proposed system to utilize the excitation-response bifurcation jumps analytically demonstrated in Fig. 2 without concern of two-way coupling influences.

We then evaluate the sensitivity of the system to periodic input voltage V_i to determine best constant-frequency operating conditions for which to utilize bifurcation for sensing objectives. Due to the above validation that structure-transducer influences are one-way, the circuit bifurcation dynamics may be comprehensively mapped by supplying a controlled input voltage V_i with the bistable circuit disconnected from the piezoelectric transducer leads.

Fig. 5 plots the magnitude of the measured bistable circuit output voltage frequency response frf (frf) which is the ratio of bistable output voltage V_o cross-spectrum to input voltage V_i autospectrum. A function generator supplies forward-swept input voltage with incrementally increasing amplitude following each sweep. Lines of constant phase lag to the excitation are indicated. The dotted line in Fig. 5 indicates approximate demarcation between low- and high-energy response regimes. Increasing darkness of the contour represents greater frf magnitude. At the transition between low- and high-energy dynamic regimes, an abrupt change in response amplitude is observed. A key operational area is observed in Fig. 5 denoted by the dashed line, where we may excite the bistable circuit at fixed frequency around 10 Hz and use amplitude shifts caused by changing input voltage level to cross the bifurcation and yield a sudden response magnitude difference. In light of the validated equation system (1), changes in input voltage V_i level may be representative of fixed base excitation (or direct forcing) characteristics but varying structural parameters m, b, or k.

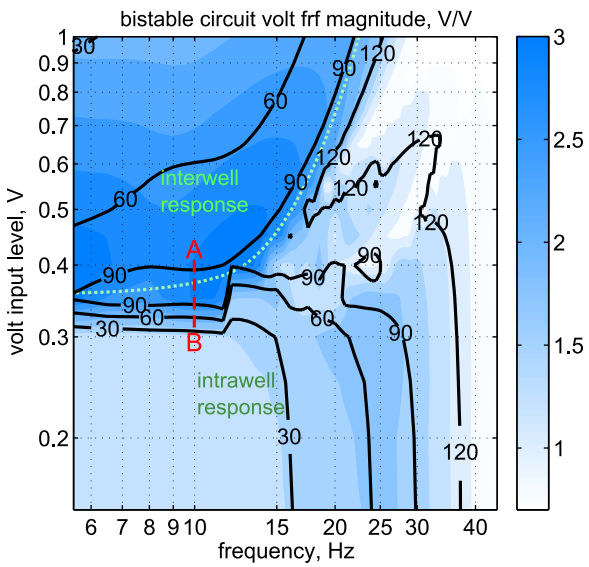

FIG. 5. Experimental bistable circuit output voltage frf magnitude with lines of constant frf phase lag (degrees). Dotted line represents approximate measured transition from low(intrawell)-to-high(interwell) energy oscillations.

Having identified a favorable bistable circuitry operating area for bifurcation-based sensing as shown in Fig. 5, the complete experimental setup of Fig. 1 is then employed. The experiments demonstrate the ability of changing structural mass to yield an input level change to the circuit and consequently induce successive bifurcation phenomena. The system is excited at 9.82 Hz which is less than the baseline structural natural frequency 9.90 Hz. Thus, increased beam mass decreases the natural frequency and amplifies beam response X at 9.82 Hz. After a certain mass accumulation, the natural frequency is reduced to a degree that excitation at 9.82 Hz is then *above* resonance causing beam response (and hence circuit input level V_i) to decrease due to continued added mass. In this way, we demonstrate the full excitation level-response amplitude trajectory exhibited in Fig. 2(a), first by upward jump in bistable circuit response, D-E, and thereafter the sudden drop down, G-H. This is also similar to following trajectory B-A-B in Fig. 5.

The beam is then excited at 9.82 Hz with arbitrary excitation level and we select input resistance R_i to tailor input voltage V_i such that the circuit output voltage exhibits intrawell dynamics near the bifurcation, close to the operational state indicated by point B in Fig. 5. Adjustment of R_i is a primary means to tailor the detection sensitivity, i.e., initial nearness to bifurcation. Wax masses are weighed and incrementally applied to the beam tip. Following each mass addition, we evaluate the structural natural frequency and damping ratio, measure the bistable circuit output voltage V_o, and disconnect the bistable circuit to measure voltage across resistor R_i (*direct* output) for comparison of response amplitudes. The voltage autospectra at 9.82 Hz are normalized with respect to data taken without added mass.

Fig. 6 presents the changing response characteristics as functions of added mass ratio which is wax mass accumulation normalized to baseline structural mass. Fig. 6(a) shows that damping ratio change exhibits no correlation to mass addition, while natural frequency decreases in consequence to accumulated mass although not uniformly. In Fig. 6(b), both direct and bistable circuit output responses initially increase by comparable degrees due to mass accumulation. However, once added mass ratio of 0.0034 is reached, excitation at 9.82 Hz is much closer to the reduced natural frequency of the system, causing greater beam vibration levels and therefore input voltage V_i; consequently, with increase of mass ratio to 0.0036, the bistable circuit crosses a bifurcation to yield a sudden jump in response providing for sensitive detection of the small parameter change. Following continued increase of mass, resulting in above-resonance excitation, the bifurcation drop at mass ratio 0.0114 is reached. Thus, net mass accumulation of ratio 0.0078 is *passively* detected via successive jumps; other bifurcation-based sensing strategies necessitate tracking hardware to obtain such measurements. With careful design of the circuit in relation to structural parameters, the specific accumulated mass addition required to traverse points E^* to G^* may be modified. Thus, the proposed system offers not only highly sensitive detection of fine incremental mass addition near bifurcations themselves but also a means to monitor specific quantities in a purely passive manner. Fig. 6 demonstrates a significantly enhanced, unambiguous, and passive detection of mass

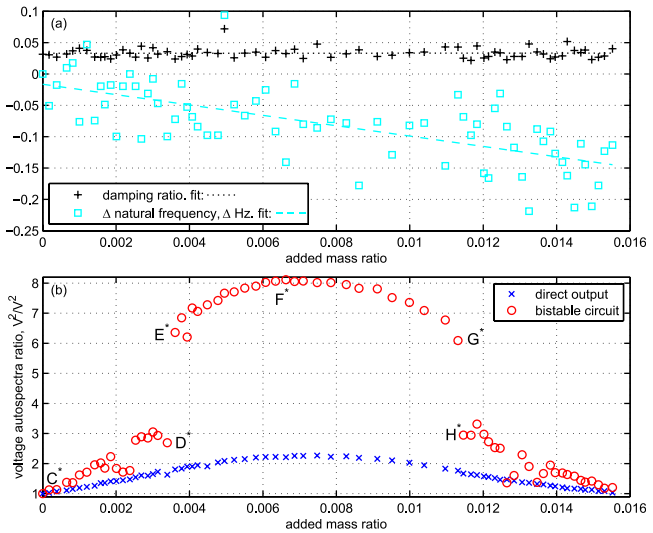

FIG. 6. (a) Structural natural frequency and damping ratio change. (b) Voltage autospectra at 9.82 Hz normalized to case of no added mass. Letter locations correspond to similar response points in Fig. 2(a) bifurcation curve.

change as compared to the small and non-uniform reduction of natural frequency which it induced.

There are several advancements and opportunities provided by the proposed bifurcation-based sensing methodology. The approach utilizes the integration of a bistable electric circuitry to enable highly sensitive detection of structural change, while the sensitivity of monitoring natural frequency shift suffers due to uncertainty and noise. By using electrical jump events, a microscale implementation of the method requires only a conventional MEMS resonator, thus simplifying the total system by isolating complex nonlinear dynamics to an easily tailored electrical system not subject to fatigue. Additionally, the features of the approach are well-suited for the introduction of bifurcation-based sensing into the structural health monitoring field where mechanical nonlinear dynamics are less pervasive and natural frequency shift may be an unreliable indicator of change. Since the influence of the structure-transducer upon the circuit is ideally a pure input voltage, the sensitivity is easily tailored by adjusting input resistor R_i, which is desirable to eliminate false positives caused by operating too close to bifurcation. As compared to past bifurcation-based MEMS sensing approaches having a uni-directional jump event to exploit for mass accumulation, the proposed protocol provides *multiple* jump events that may be used sequentially to denote pre-determined quantities of change. This is a degree of robustness and versatility not obtainable with existing bifurcation-based sensing methods. In summary, by exploiting bistable dynamics in a purely electrical form, the proposed methodology greatly enhances the versatility of bifurcation-based sensing and extends its range of applicability to fields previously not regarded.

[1]T. Thundat, E. A. Wachter, S. L. Sharp, and R. J. Warmack, Appl. Phys. Lett. **66**, 1695 (1995).
[2]H. Sohn, C. R. Farrar, F. M. Hemez, D. D. Shunk, D. W. Stinemates, B. R. Nadler, and J. J. Czarnecki, LANL Report LA-13976-MS, 2004.
[3]L. J. Jiang, J. Tang, and K. W. Wang, Smart Mater. Struct. **15**, 799 (2006).
[4]R. Vijay, M. H. Devoret, and I. Siddiqi, Rev. Sci. Instrum. **80**, 111101 (2009).

[5]W. Zhang and K. L. Turner, Sens. Actuators, A **122**, 23 (2005).
[6]C. B. Burgner, K. L. Turner, N. J. Miller, and S. W. Shaw, in *Solid-State Sensors, Actuators, and Microsystems Workshop, Hilton Head Island, South Carolina* (2010), p. 130.
[7]Z. Yie, M. A. Zielke, C. B. Burgner, and K. L. Turner, J. Micromech. Microeng. **21**, 025027 (2011).
[8]M. I. Younis and F. Alsaleem, J. Comput. Nonlinear Dyn. **4**, 021010 (2009).
[9]V. Kumar, J. W. Boley, Y. Yang, H. Ekowaluyo, J. K. Miller, G. T.-C. Chiu, and J. F. Rhoads, Appl. Phys. Lett. **98**, 153510 (2011).
[10]R. Lifshitz and M. C. Cross, *Reviews of Nonlinear Dynamics and Complexity*, edited by H. G. Schuster (Wiley, Weinheim, 2008), Vol. 1, pp. 1–52.
[11]K. W. Wang and J. Tang, *Adaptive Structural Systems with Piezoelectric Transducer Circuitry* (New York, Springer, 2008).
[12]R. L. Harne, M. Thota, and K. W. Wang, Appl. Phys. Lett. **102**, 053903 (2013).
[13]A. Tamaševičius, G. Mykolaitis, V. Pyragas, and K. Pyragas, Phys. Rev. E **76**, 026203 (2007).
[14]P. Holmes, Philos. Trans. R. Soc. London, Ser. A **292**, 419 (1979).
[15]N. E. duToit, B. L. Wardle, and S. G. Kim, Integr. Ferroelectr. **71**, 121 (2005).
[16]*The Duffing Equation: Nonlinear Oscillators and their Behaviour*, edited by I. Kovacic and M. J. Brennan (Wiley, Chichester, 2011).
[17]S. S. Rao, *Mechanical Vibrations* (Pearson Prentice Hall, Upper Saddle River, 2004).